

Cantori and dynamical localization in the Bunimovich Stadium

Fausto Borgonovi^[a,b,c], Paolo Conti^[d], Daniela Rebuzzi^[d], Bambi Hu^[e,f], and Baowen Li^[e]

^[a] *Dipartimento di Matematica e Fisica, Università Cattolica, via Trieste 17, 25121 Brescia, Italy*

^[b] *Istituto Nazionale di Fisica Nucleare, Sezione di Pavia, via Bassi 6, 27100 Pavia, Italy*

^[c] *Istituto Nazionale di Fisica della Materia, Unità di Milano, via Celoria 16, 22100 Milano, Italy*

^[d] *Dipartimento di Fisica Nucleare e Teorica, Università di Pavia, via Bassi 6, 27100 Pavia, Italy*

^[e] *Department of Physics and Centre for Nonlinear Studies, Hong Kong Baptist University, Hong Kong, China*

^[f] *Department of Physics, University of Houston, TX77204, USA*

Classical and quantum properties of the Bunimovich stadium in the diffusive regime are reviewed. In particular, the quantum properties are directly investigated using an approximate quantum map. Different localized regimes are found, namely, perturbative, quasi-integrable (due to classical Cantori), dynamical and ergodic.

PACS numbers: 05.45+b

I. INTRODUCTION

Long time ago, some physicists in the Siberian winter were playing dice with chaos and quantum mechanics. This game resulted in a paper which has been quoted $N+1$ times in literature¹ and which is known as a milestone in Quantum Chaos.

Far from being an isolated branch of physics, Quantum Chaos has revealed its importance in the last twenty years in many important physical applications of different fields: Solid State, Nuclear, Atomic and Mesoscopic physics, just to give few examples.

The common paradigm in Quantum Chaos is the so-called Kicked Rotator Model (KRM) whose dynamics is described by the Chirikov standard map (CSM). It represents the safe retreat of many researchers working in Quantum Chaos. Indeed, even if still now papers dealing with some hidden property of the Chirikov Standard Map appear², (after the monumental work of Boris Chirikov published in 1979³), or regarding new mathematical advances in the knowledge of the Floquet spectrum of the KRM⁴, we may say that its general behavior is quite well understood, at least from the physical point of view.

In this paper we show how a different physical problem can be explained using old results borrowed from KRM.

The model under current investigation is the Bunimovich Stadium⁵. The properties of this model are well known in literature, both from physical and mathematical point of view. Here we are interested in this particular billiard, characterized by a straight line $2a$ much smaller than the semicircle radius R : $\epsilon = a/R \ll 1$. Preliminary studies⁶ have shown that the classical motion in the angular momentum is diffusive and it can be conveniently described by a 2-d area preserving map. In the same paper⁶ the study of the nearest neighbor level spacing distribution (NNLSD) exhibits a different behavior depending on the energy range where the statistics is taken. In particular, at fixed $\epsilon \ll 1$ the NNLSD shows a smooth crossover from a Poisson to a Wigner-Dyson distribution as the energy is increased. The borders below and above which one can expect a particular distribution were theoretically predicted and confirmed by numerical data⁶.

The region characterized by intermediate statistics⁷ can be associated, on the basis of a well defined picture^{7,8}, with the presence of dynamical localization. In a sense, the qualified adjective “dynamical” was, at that stage quite inappropriate. Indeed only and indirect proof of dynamical localization were given, based on level statistics. The first example of localized eigenstates, in the angular momentum basis, was given in⁹ for a rough deformation of a circular billiard. In this case, due to the finite number of harmonics describing the smooth modification of the boundary, direct exponential localization was found and the equality between quantum localization length and classical diffusion rate established.

In this paper we enforce this viewpoint by studying directly the quantum dynamics instead of eigenfunctions and eigenvalues. This can be efficiently realized, from the numerical point of view, only quantizing the classical map. The obtained numerical data¹⁰ indicate that quantum equilibrium distributions, differently from the classical ones, are algebraically localized in the angular momentum space. Further numerical investigations¹¹ of the stadium eigenfunctions confirmed their algebraic localization in the in angular momentum space. Nevertheless it is possible to distinguish among different quantum regimes.

Besides the perturbative regime, characterized by trivial periodic dynamical behavior, other different kind of localization can be identified. The first one, called quasi-integrable, has been associated to classical Cantori. Another one is marked by dynamical localization, despite the algebraic localized distribution (with this word we mean a situation in which classical diffusion rate and quantum localization length have the same numerical value). Recent analytical studies¹² support this analysis.

The paper is organized as the following: in section II we consider the classical dynamics inside the Bunimovich stadium as given by a suitable perturbed twist map. Classical properties of the discontinuous map are then investigated in section III, while section IV is devoted to its quantum properties. Finally in section V the estimates about different borders in the energy-parameter

plane are summarized.

II. MAPPING THE BUNIMOVICH STADIUM

The ensemble dynamics of classical point particles having energy E , unit mass and initial angular momentum l_0 , colliding elastically inside the Bunimovich Stadium is described, when $\epsilon \ll 1$, by the following map ($R = 1$)⁶

$$\begin{aligned}\bar{l} &= l - 2\epsilon \sin \theta \operatorname{sgn}(\cos \theta) \sqrt{2E - l_0^2} \\ \bar{\theta} &= \theta + \pi - 2 \operatorname{asin}(\bar{l}/\sqrt{2E}) \quad \text{mod } -2\pi\end{aligned}\quad (1)$$

In (1) θ is the angle measured from the center of the Stadium, l the angular momentum measured from the same center and the overlined variables $(\bar{\theta}, \bar{l})$ indicate the values taken after the collision with border. This map has been obtained by neglecting collisions with the straight lines, terms $O(\epsilon^2)$ and in the local approximation (small variations in the angular momentum). Indeed, it is easy to understand that while in the first equation of (1) l can grow infinitely, the second equation loses its validity when $|l|$ approaches its maximum value $\sqrt{2E}$. The existence of such a bound is a trivial consequence of the energy conservation.

If we now put $l_0 = 0$ and approximate $\operatorname{asin}(x)$ with its argument (since we must exclude the values $|x| \simeq 1$), we get:

$$\begin{aligned}\bar{l} &= l + k \sin \theta \operatorname{sgn}(\cos \theta) \\ \bar{\theta} &= \theta + T\bar{l} \quad \text{mod } -2\pi\end{aligned}\quad (2)$$

where we put $k = 2\epsilon\sqrt{2E}$, $T = 2/\sqrt{2E}$, $l \rightarrow -l$ and π has been neglected since $\sin \theta \operatorname{sgn}(\cos \theta)$ is π -periodic. Map (1) has been obtained⁶ for $\epsilon \ll 1$, therefore (2) holds when $kT = 4\epsilon < 1$. The case $kT > 1$, which represents a possible regime for (2) has no physical meaning here and it will not be taken into account.

Map (2) on the cylinder $[0, 2\pi) \times (-\infty, \infty)$ has been recently investigated¹⁰ for $kT < 1$. Results can be then extrapolated to our case assuming $|l| \ll \sqrt{2E}$. In the next sections we present a detailed study of classical and quantum properties of map (2).

III. DISCONTINUOUS TWIST MAPS

Let us write (2) by introducing the variables $J = lT$, $K = kT$ in the following way :

$$\begin{aligned}\bar{J} &= J + K \sin \theta \operatorname{sgn}(\cos \theta) \\ \bar{\theta} &= \theta + \bar{J} \quad \text{mod } -2\pi\end{aligned}\quad (3)$$

such that we have single parameter K . Map (3) belongs to a particular class of discontinuous twist maps. We use the word "discontinuous" to mark the difference

with the Chirikov Standard Map, for which $\bar{J} - J = K \sin \theta$ is a continuous function in the interval $[0, 2\pi)$.

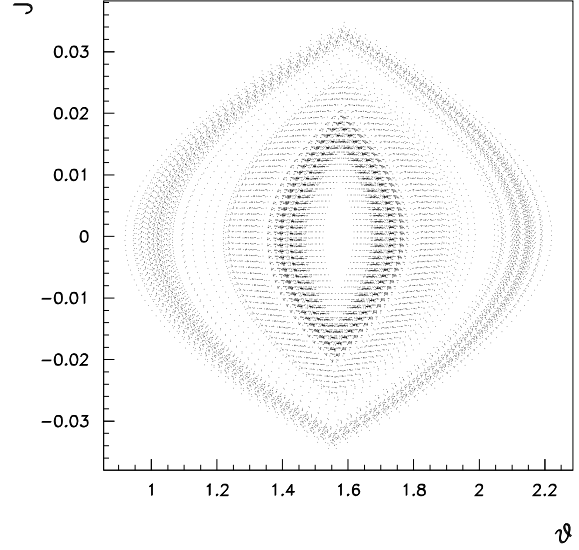


FIG. 1. Poincaré surface of section for map (3) and $K = 0.001$. One particle has been iterated $2 \cdot 10^4$ times.

The most studied case in the set of discontinuous functions is the saw-tooth map (STM) where the change in the angular momentum is given by $\bar{J} - J = K(\theta - \pi)/\pi$. For this map the classical transport properties have been studied, quite long ago¹³. The relevant difference of the STM, if compared with the CSM, is characterized by the absence of a KAM structure. Indeed, since the hypothesis of KAM theorem are not satisfied, we do not expect KAM tori exist for any K value, independently from its smallness. Namely, differently from the CSM, where for $K < 1$ the motion is typically regular on invariant tori, here one finds absence of KAM tori for any K ; nevertheless, invariant structures still exist. Indeed Cantori can be defined in the same way as in the STM¹³. An example of the motion in the neighborhood of Cantori is shown in Fig.1. As one can see the motion is far from being chaotic even if, upon the increasing of time, a single orbit can explore, in a dense way, the whole phase space. Moreover, the resulting motion is conveniently described by a diffusive equation for the distribution function as can be inferred by looking at the behavior in time of the average squared momentum (see Fig.2a).

The linear growth in time, after a transient time (see Fig.2) and the corresponding Gaussian distribution in angular momentum, at a given time, (see for instance⁶) are usually taken as a common reference for the existence of a diffusive motion³.

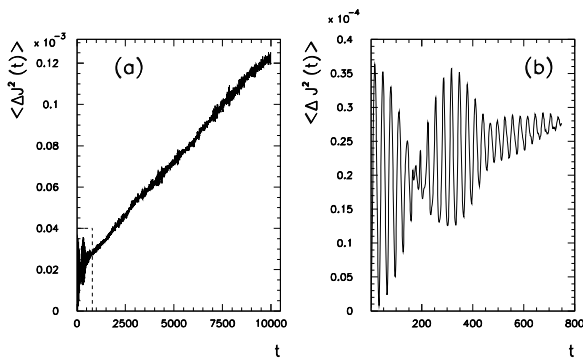


FIG. 2. Growth of the average momentum spreading in time for the discontinuous map (3) at $K = 0.001$. b) is a magnification of the small area indicated among dashed lines in the left corner of a). The initial ensemble consists of 2000 particles having the same momentum $J_0 = 0.1$ and random phases θ .

For such discontinuous maps, the resulting coefficient diffusion, (extracted numerically from a linear fit of Fig.2a), can be shown to depend on the parameter K in the following way^{13,6,10}:

$$\mathcal{D} = \lim_{t \rightarrow \infty} \langle \Delta J^2(t) \rangle / t \propto K^{5/2} \quad (4)$$

where t is the iteration time.

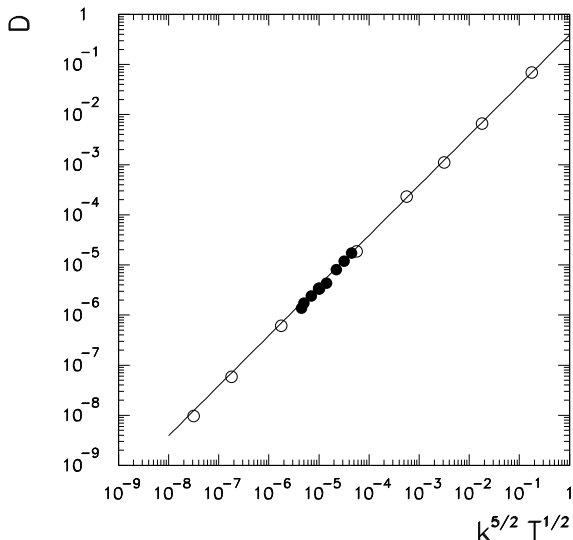


FIG. 3. Diffusion rate for the discontinuous map (2) for different k and T versus $k^{5/2}T^{1/2}$. Open circles are for $T = 1$, full circles for $k = 0.01$; both for $kT < 1$. Full line is the best fit line $\mathcal{D} = 0.39k^{5/2}T^{1/2}$.

In terms of the original variables one get $\mathcal{D} = \langle \Delta l^2(t) \rangle / t \propto k^{5/2} \sqrt{T}$ (see Fig.3). The regime characterized by a diffusion coefficient scaling as $K^{5/2}$ has been called slow diffusion¹⁰. This mark the difference from the standard quasilinear regime ($K > 1$) where typically one has $\mathcal{D} \simeq K^2$ (superimposed to oscillations¹⁴).

The dependence on the power $5/2$ has been explained¹³ in terms of a transport model based on a Markovian partition of the phase space for the STM and it clearly indicates that the random phase approximation³ cannot be applied in this case.

Phases are indeed correlated within a time τ (see Fig.2 b) during which the resulting motion cannot be chaotic nor diffusive. A correct evaluation of this time scale could be a key in understanding the “strange” exponent $5/2$, even if numerically it is quite difficult to obtain sharp results.

IV. QUANTUM MAP DYNAMICS

Now we turn to the quantum analysis. Adopting the nowadays standard procedure¹ we analyze the quantum evolution of map (2) by means of the one-period evolution operator given explicitly by ($\hbar = 1$):

$$\mathcal{U}_T = e^{-iT\hat{n}^2/2} e^{-ik|\cos\theta|} \quad (5)$$

where $\hat{n} = -i\partial/\partial\theta$. Apart from the modulus in the potential $V(\theta) = |\cos\theta|$ the evolution operator \mathcal{U}_T is exactly the same as the Kicked Rotator one. Anyway the presence of the modulus leads to many important physical differences. Indeed, written in the momentum basis n , the matrix elements $\mathcal{U}_{n,m} = \langle n | \mathcal{U}_T | m \rangle$ decay as a power law $|\mathcal{U}_{n,m}| \sim 1/|n-m|^2$ away from the principal diagonal (and not faster than exponentially as for the KRM). This case has been investigated for banded random matrices²⁰, where it was shown that eigenfunctions are also algebraically localized with the same exponent.

The presence of power law localized eigenstates has major consequences. First of all it is not, a priori, obvious if the mechanism connected with the exponential dynamical localization holds even in this case. Moreover, while in case of exponential localization a unique measure of localization is defined (up to a constant), for algebraical localization different definitions of localizations can, in principle, give rise to different parametric dependences.

Here we consider, as a measure of the degree of localization, the variance ξ_σ of the stationary distribution $P(n) = |\psi_n(t \rightarrow \infty)|^2$:

$$\xi_\sigma = \left[\sum_n n^2 P(n) \right]^{1/2} \quad (6)$$

which we expect to have a well defined classical limit.

A. The Kicked Rotator Model for $kT < 1$

Before we turn to numerical results, it is useful to consider, as a common reference, the KRM. This is far from being pedagogical, since the case we are interested in here ($kT < 1$) has not been an object of intense investigations in the past. Moreover, in this region, characterized by

classical regular motion, it is quite difficult to get homogeneous results. For instance, one should expect that the localization length of the stationary distribution strongly depend on the initial conditions. Starting within a regular region (stable island around periodic orbits) would result in a spreading width surely not larger than the size of the island (excluding the exponentially small tunneling among different classical tori). This was indeed what Shepelyansky¹⁸ found: the spreading of the quantum stationary distribution can be roughly identified with the width $\simeq \sqrt{k/T}$ of the main classical resonance, whose size is $\sqrt{k/T}$, when $kT < 1$. Another result was obtained again by Shepelyansky by investigating directly the quasi-energy eigenfunctions¹⁹: he found direct proportionality between their localization lengths and the parameter k : $\ell \simeq k/4$. The different regimes in this undercritical case were also reported by Izrailev⁷. According to his Fig.3 (see also text) the case $K = kT < 1$ is marked by two different quantum borders. One is the condition for the applicability of common perturbative theory ($k \simeq 1$) while the other one is the condition for the semiclassical approach to describe quasiperiodic or chaotic motion (Shuryak border $k \simeq T$). When $k < T$ the size of the nonlinear resonance is less than the distance between neighboring unperturbed levels and the quasiperiodic classical behavior is suppressed by quantum effects.

Our data on the behavior of ξ_σ confirm and extend this general picture. They can be summarized as follows:

1) ξ_σ depends, for $K = kT < 1$, only on the scaling parameter k/T .

2) as a function of k/T two different regimes can be numerically detected, one linear, when $k < T$ (below the Shuryak border) and another, for $k > T$, where $\xi_\sigma \propto \sqrt{k/T}$.

These results are presented in Fig.4.

As one can see the scaling law is accurate up to eight orders of magnitude. The intersection point between the two lines ($k \simeq T$ called Shuryak border), is the only transition point (for ξ_σ) we are able to detect numerically. Results have been checked to be independent from the choice of the initial state $\psi_n = \delta_{n,n_0}$. Since typically the variance $\xi_\sigma(t) = \sqrt{\langle \Delta n^2(t) \rangle}$ is an oscillatory function of the iteration time t (quasi-periodic motion) the average (in time) value has been taken. Fluctuations are typically quite large, often on the same order of the average value. On the basis of previous results we identify two different regimes, for the KRM in the classically regular case $kT < 1$: the perturbative one $\xi_\sigma \simeq k/T$ and the quasi-integrable one $\xi_\sigma \simeq \sqrt{k/T}$.

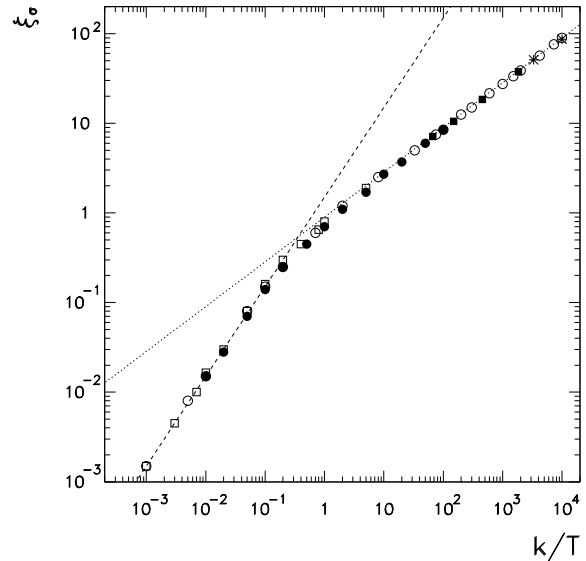


FIG. 4. Localization length as a function of the scaling parameter k/T for the Kicked Rotator and $kT < 1$. Full symbols are obtained by fixing k and varying T : circles ($k = 0.01$), squares ($k = 1$), asterisks ($k = 10$). Open symbols are obtained by fixing T and varying k : circles ($T = 0.01$), squares ($T = 0.1$). Dashed line is $1.5k/T$ (linear regime), while dotted line is $0.9\sqrt{k/T}$.

B. The discontinuous quantum model in the slow diffusive case

In this section we analyze the quantum behavior of the discontinuous map (2). The classical map is a good approximation to the real billiard dynamics only for $\epsilon = kT/4 \ll 1$. This means that we should consider, as a physical regime, only the slow diffusive one. The condition of applicability $|l|/\sqrt{2E} < 1$ will be considered in details in section V.

Iteration of the quantum map (5) in this regime typically gives rise to the second moment $\langle \Delta n^2(t) \rangle$ which is an oscillatory function of the time t . In particular, it is possible to characterize values of the parameters k and T which leads to periodic or irregular oscillations. In Fig.5 we show, for different k and T , the behavior of ξ_σ in time. As dashed lines we indicate the average values over few oscillation periods. We will back to this picture later on when we discuss the different quantum regimes.

By varying k and T and taking ξ_σ as in Fig.5, we obtain three different scaling regions: the first one for $k < T$ in which $\xi_\sigma \simeq k/T$, a second one for $1/\sqrt{T} > k > T$ characterized by $\xi_\sigma \simeq \sqrt{k/T}$ and the third one, for $1/\sqrt{T} < k < 1/T$, in which $\xi_\sigma \simeq D$ (see Fig.6).

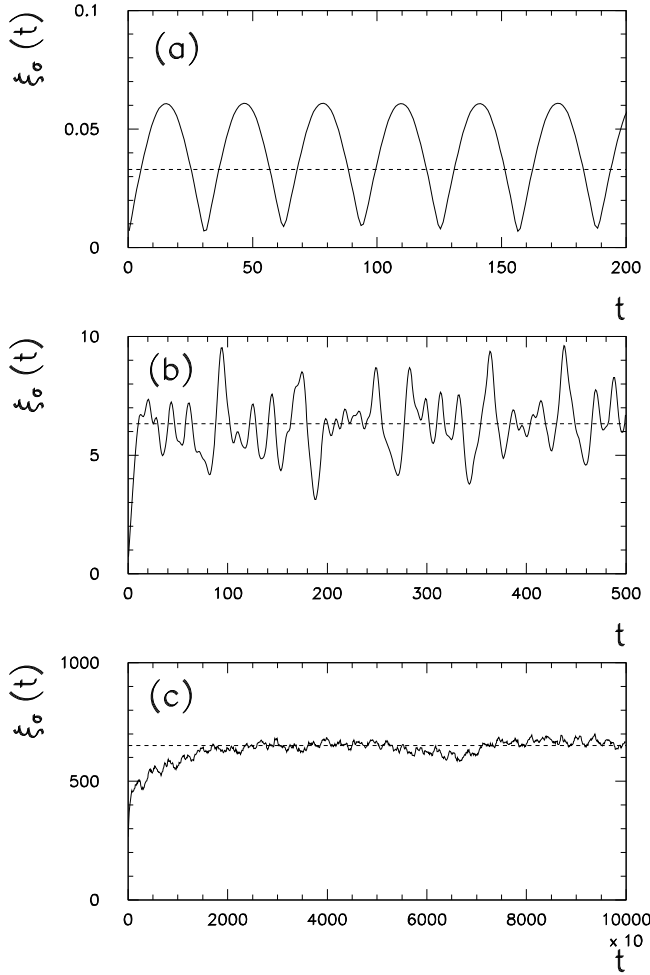


FIG. 5. Wave packet spreading as a function of the iteration time t . Here $\xi_\sigma(t) = [\sum_n n^2 |\psi_n(t)|^2]^{1/2}$ (a) is for $k = 0.01$ and $T = 0.1$ (perturbative region), dashed line is the average $\xi_\sigma = 0.033$; (b) is for $k = 1$ and $T = 0.01$ (quasi-integrable region), dashed line is the average $\xi_\sigma = 6.33$; (c) is for $k = 100$ and $T = 0.001$ (dynamical localization region), dashed line is the average $\xi_\sigma = 650$.

It is easy to identify the first two regions in close analogy with those found for the KRM (see previous subsection). While the existence of a perturbative region with the same characteristics of the KRM is not surprising, much care must be taken in interpreting the quasi-integrable region. Indeed, while for the KRM we may properly speak about width of classical resonance, in this case we have no classical resonances at all. Nevertheless a close inspection of Fig.1 indicates the presence of islands of “quasi-integrability” which means that trajectories spend a lot of time before leaving from them. This region is indeed dominated by classical Cantori, which act, from the quantum point of view as total barriers to the motion. These effects, namely the quantum propagation through classical Cantori have been investigated in Ref.^{21–23}. In particular, a relation between width of the holes of Cantori and \hbar should exist, in order to obtain a

meaningful semiclassical limit. For instance Mackay and Meiss proposed²³ that Cantori could act as proper tori if the flux exchanged among different turnstiles is less than \hbar .

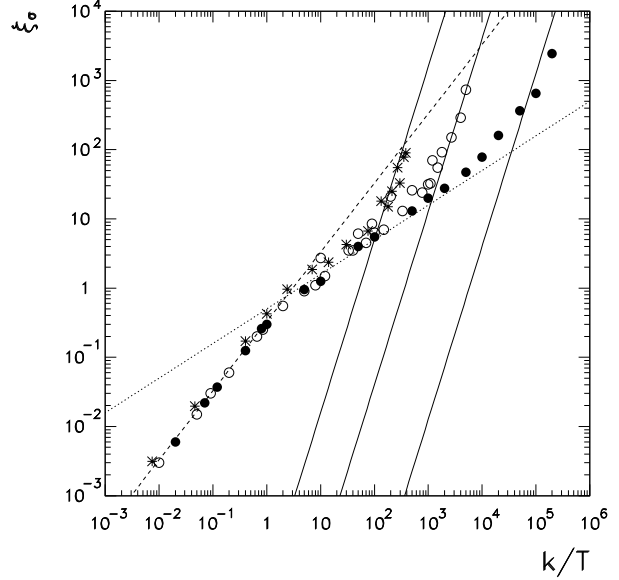


FIG. 6. Localization length ξ_σ as a function of k/T . Three different sets of cases are shown, each one keeping T fixed and varying k : full circles ($T = 0.001$), open circles ($T = 0.01$) and asterisks ($T = 0.05$). Dashed line is $k/3T$ while dotted is $\sqrt{k/T}/2$. Full lines are $\xi_\sigma = D(T)$ for the three different sets, from the left to the right $T = 0.05, 0.01, 0.001$.

Let us now analyze in more details the existence of a third scaling region for the localization length. The classical analog of these quantum regions of localizations is a diffusive regime (after a transient time). Nevertheless the localization found is not “dynamical” in the sense that it cannot be derived for instance by taking the approach used by Chirikov, Izrailev and Shepelyansky for the KRM²⁴. Moreover, since this kind of localization is shared by the KRM, whose classical counterpart is regular motion, it cannot be followed by classical diffusive excitation. A look at Fig.5 a-b confirms this view.

On the other side, if the typical relation of the dynamical localization $l_\sigma \simeq D$ holds true, the diffusion rate, in order to produce an initial quantum classical-like diffusive spreading, has to be larger than the size of the classical “quasi-resonance”. This in turn allows us to estimate the second transition point as follows:

$$D = D_0 k^{5/2} \sqrt{T} = c \sqrt{k/T} \quad (7)$$

which gives $k_{cr} = \sqrt{c/D_0 T}$ (where c and D_0 are numerical constants of order one. One can then guess that, if any, the dynamical localization regime can exist for $k > k_{cr} = \sqrt{c/D_0 T}$.

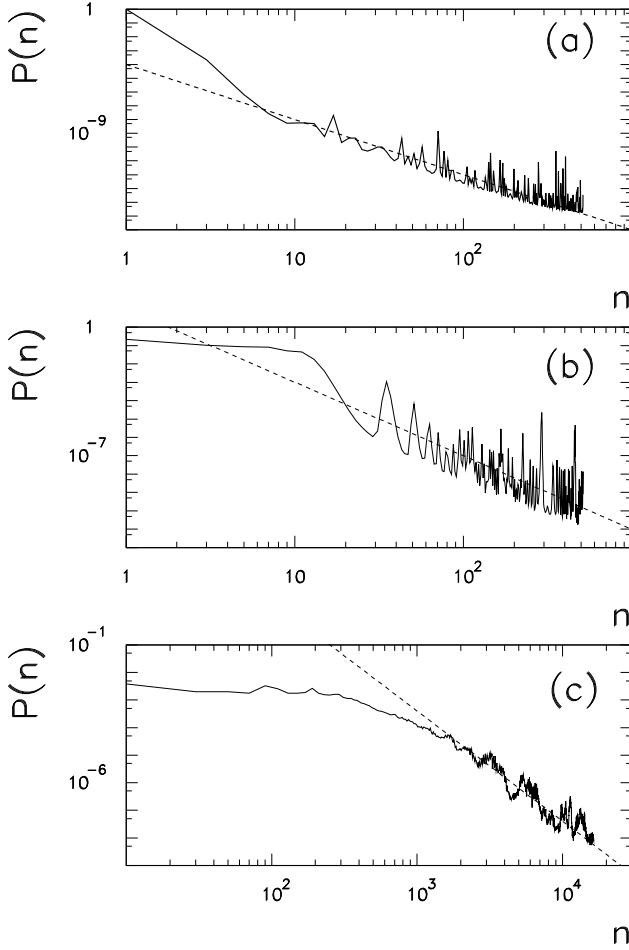


FIG. 7. Stationary distribution averaged over few oscillation periods as a function of the momentum n . (a) is for $k = 0.01$ and $T = 0.1$ (perturbative region) (b) is for $k = 1$ and $T = 0.01$ (quasi-integrable region) (c) is for $k = 100$ and $T = 0.001$ (dynamical localization region). Lines represent the power $1/n^4$ and are shown to guide the eye.

Our numerical computations indicate that the dynamical localization regime indeed exists, as can be inferred from Fig.6. The sharp rise of the full lines shown in Fig.6, (one for each T since the diffusion rate depends on T) indicates, without any doubt, the validity of the previous picture and the existence of the critical points, $k \simeq T$ and $k \simeq 1/\sqrt{T}$.

The existence of these thresholds for the Bunimovich stadium, and the regime of quasi-integrability as well, has been confirmed analytically by Prange, Narevich and Zaitsev¹². Indeed they were able to find an analytical expression for the eigenfunctions up to $\epsilon\sqrt{E} \simeq 1$, which in terms of map variables reads $k \simeq 1/\sqrt{T}$. Above the threshold $\epsilon\sqrt{E} \simeq 1$ the semiclassical perturbative approach fails. According to our point of view this represents the k value necessary to start the classical-like diffusion process in presence of slow diffusion.

Let us add few comments about the shape of the stationary distribution. In all cases we have found good agreement with a power law distribution $P(n) \simeq |n - n_0|^{-4}$. In Fig.7 we show the correspondent stationary distributions for the cases of Fig.5. The lines, indicating the power law behavior, are drawn to guide the eye. This means that results obtained from banded random matrices²⁰ can be extrapolated even when both randomness and dynamical chaos are absent (perturbative and quasi-integrable regions).

The presence of power law localized states for the discontinuous map, also recently confirmed in¹¹ for the stadium eigenfunctions, should be somehow put in relation with the exponential localization found in⁹ for the eigenfunctions of a rough billiard. This peculiarity should be in turn related with the particular boundary shape perturbation. Indeed, while in the rough billiard considered in⁹, a finite number M of harmonics is necessary in order to produce the deformation from the circle, the stadium boundary perturbation is not analytical. The classical rough map is shown⁹ to be chaotic when $\epsilon > \epsilon_c \sim M^{-5/2}$. It is then clear that when $M \rightarrow \infty$ KAM regular structures disappear and the situation depicted by the discontinuous map appears.

To end this section let us remark that a similar behavior happens if another definition of localization length is taken. In Fig.8 we show the inverse participation ratio of the quantum distribution $i\text{pr} = 1/\sum_n |\psi_n|^4$ as a function of the scaling parameter k/T . The absence of a perturbative region is due to the fact that, by definition, $i\text{pr} \geq 1$. Moreover, let us note that a numerical constant has to be added in order to follow numerical data. Namely, the dynamical localization regime is marked by $i\text{pr} \simeq D/4$. The simple proportionality between l_σ and $i\text{pr}$, even if not surprising (the same happens for the KRM), has to be considered accidental for power law localized distributions.

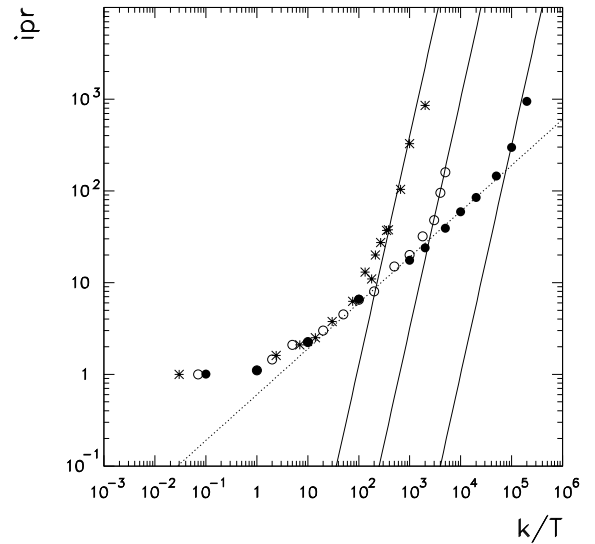


FIG. 8. Inverse participation ratio ipr as a function of k/T . Three different sets of cases are shown, each one keeping T fixed and varying k : full circles ($T = 0.001$), open circles ($T = 0.01$) and asterisks ($T = 0.05$). Dotted line is $0.6\sqrt{k/T}$. Full lines are $ipr = D(T)/4$ for the three different sets, from the left to the right $T = 0.05, 0.01, 0.001$.

V. BORDERS FOR THE STADIUM

The results found in the previous sections can be extended to the Bunimovich Stadium. This will lead to important estimates which enable us to discriminate between different physical situations. In particular the critical points found previously give rise to relations between the energy and the small parameter ϵ .

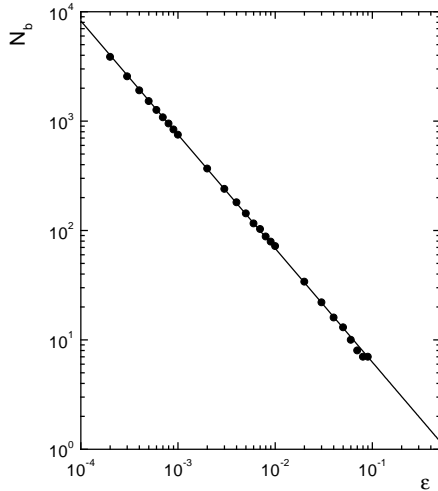


FIG. 9. Perturbative border for the Bunimovich Stadium. N_b is the quantum number corresponding to the eigen energy E . Solid circles represent numerical data, and straight line is the best-fit $N_b = 0.57/\epsilon^{1.04}$.

The first regime (perturbative), is characterized by $k < T$ or $2E\epsilon < 1$. From the billiard point of view this means that levels having an energy less than $E \sim 1/\epsilon$ can be obtained perturbatively from those of the unperturbed spectrum ($\epsilon = 0$, e.g. the circle). The numerical study of the energy spectrum gives a confirmation for this border. We label the energy levels as $E_N(\epsilon)$. If ϵ is sufficiently small we can assume the shift $\Delta E = E_N(\epsilon) - E_N(0)$ to be quite small. On the other hand the energy spectrum is characterized by an average level spacing δE_N which is given approximately by the Thomas-Fermi formula²⁵:

$$\delta E_N \simeq \frac{E_N}{N_b} \simeq \frac{8\hbar^2}{mR^2} \quad (8)$$

where $m = 1$ is the particle mass, $R = 1$ is the circle radius and N_b is the number of levels up to energy E . In order to be in a perturbative regime there should be no levels overlapping, namely $\Delta E_N(\epsilon) < \delta E_N$. This gives a relation between the energy E (or the level number

N_b) and the small parameter ϵ , which can be detected numerically. We show our numerical results in Fig.9. The best fit gives rise to $0.57/\epsilon^{1.04}$, which is in a good agreement with the theoretical prediction. Numerically, N_b is obtained by comparing the eigenenergy list of the circular billiard and that of the perturbed Bunimovich stadium of ϵ .

Moreover, a kind of semiclassical approach is possible¹² up to $k = 1/\sqrt{T}$, or $E \sim 1/\epsilon^4$ (we omit a numerical constant in front of this expression : its value can be obtained only numerically). This means that the analytical approach to eigenvalues and eigenvectors is possible up to this energy value. Nevertheless, as soon as the map dynamics correctly approximates the real dynamics, the localization length should have a different energy dependence. Even in this case a direct numerical approach is needed in order to give a definite answer.

Let us now come to the much more interesting case marked by the dynamical localization. We have found that this is possible only for $E > 1/\epsilon^4$. According to the dynamical localization theory the quantum spreading will occur up to a time $t_B \simeq D$ called break time. Following⁶ we may speak of a proper localized quantum regime only if $t_B < t_{erg}$, where t_{erg} is the classical time in order to reach a stationary ergodic distribution, estimated as $\Delta l^2 \simeq Dt_B$ or $t_B \simeq \epsilon^{-5/2}$. Would t_B be larger than t_{erg} , classical and quantum distributions will both reach an ergodic stationary distribution. Putting $t_B = t_{erg}$ or $E \sim \epsilon^{-5}$ we get the last critical point above which we expect quantum as well classical ergodicity.

The approach to ergodicity cannot be studied using this map. Indeed it represents a good approximation to real dynamics only for $t \ll t_{erg}$. This means that our results cannot be compared with those found by Frahm and Shepelyansky²⁶ about the approach to ergodicity via a Breit-Wigner regime. This is a situation characterized by eigenfunctions delocalized on the energy shell but with many strong isolated peaks of probability. The presence of isolated peaks of probability in our case (see Fig.7) is instead due to the classical phase space structure.

While the ergodicity regime has been previously investigated⁶ using the NNLSD, the existence of two different localized regimes ($\epsilon^{-1} < E < \epsilon^{-4}$ and $\epsilon^{-4} < E < \epsilon^{-5}$) has been only guessed on the basis of the similarity with the approximate map. In this case, the study of NNLSD should be probably accomplished by a direct study of eigenfunctions. This we argue, since it is not at all obvious how different kind of localization can affect the level statistics. A preliminary study in this direction can be found in¹¹.

Let us note that, in order to correctly approximate real dynamics with the map, one has to require $|l|/\sqrt{2E} < 1$, or $lT < 2$. One should then require that in both, quasi-integrable and dynamical localization regime, $\xi_\sigma T < 2$. This in turn means either

$$\sqrt{\frac{k}{T}}T = \sqrt{kT} < 2 \quad (9)$$

(which is always justified since $kT = 4\epsilon$ and $\epsilon < 1$) or

$$k^{5/2}T^{3/2} < 2$$

which reduces to

$$k(kT)^{3/2} \simeq \epsilon E^{1/2} \epsilon^{3/2} = E^{1/2} \epsilon^{5/2} < 2$$

or $E < 1/\epsilon^5$ which is the condition in order to have classical ergodicity. This is the reason why we neglect this condition in Sec. IV.

Most of the results were obtained by approximating the real quantum dynamics by means of a quantum map which is the quantum analog of a classical map approximating the classical dynamics. This kind of procedure is not new (see for instance²⁷). One may wonder if this is, at the end, close to the original model. The answer can come, of course, only from a direct numerical or experimental, analysis of the quantum dynamics of wave packets inside the billiard. Nevertheless it is significative that different approaches on the same model¹² give results in good agreement with ours.

After the completion of this work we became aware of other related works on the subject¹¹. In particular their numerical data, while confirming the existence of these regimes, indicate other different borders. However, from the map point of view, the transition at $k = T$ ($E \sim 1/\epsilon$) is very sharp, we cannot exclude numerically the presence of a further border at $k \sim T^{1/3}$ ($E \sim \epsilon^{-3}$). Indeed a close inspection at Fig.6, indicates a very smooth transition toward the line $\xi_\sigma = D$. Further numerical calculations are required in order to show if quantum map also shows this border.

VI. ACKNOWLEDGMENTS

We thank R. Prange, R.Narevich and O.Zaitsev for making their work available before publication. Discussions with G.Casati are also acknowledged. BH and BL were supported in part by the grants from the Hong Kong Research Grants Council (RGC) and the Hong Kong Baptist University Faculty Research Grants (FRG).

- ⁸ F.Borgonovi and G.Casati, to be published in “*Frontiers in Quantum Physics*”, Proceedings ICFQP-97, cond-mat/9711281.
- ⁹ K.M.Frahm and D.L. Shepelyansky, Phys. Rev. Lett. **78**, 1440 (1997); K.M.Frahm Phys. Rev B **55**, R8626 (1997).
- ¹⁰ F.Borgonovi chao-dyn/9801032
- ¹¹ G.Casati and T.Prosen cond-mat/9803340; cond-mat/9803360.
- ¹² R.E.Prange and R.Narevich, and O. Zaitsev chao-dyn/9802019.
- ¹³ I.Dana, N.W.Murray and I.C.Percival Phys.Rev.Lett. **62** (1989) 233.
- ¹⁴ B.Rechester, M .N.Rosenbluth and R.B.White, Phys.Rev. A **23**, 2264 (1981).
- ¹⁵ R.S. MacKay, J.D. Meiss and I.C. Percival, Physica **13D**, 55 (1984).
- ¹⁶ R.S.Mackay, private communication.
- ¹⁷ S.Bullett, Comm. Math. Phys. **107**, 241 (1986).
- ¹⁸ D.L.Shepelyansky, Physica D **8**, 208 (1983).
- ¹⁹ D.L.Shepelyansky Physica D **28**, 103 (1987).
- ²⁰ A.D. Mirlin, Y.V. Fyodorov, F.M. Dittes, J. Quezada and T.H. Seligman, Phys. Rev. E **54**, 3221 (1996).
- ²¹ R.C.Brown and R.E.Wyatt, Phys. Rev. Lett. **57**, 1 (1986).
- ²² T.Geisel, G.Radons and J.Rubner, Phys. Rev. Lett. **57**, 2883 (1986).
- ²³ R.S.MacKay and J.D.Meiss, Phys. Rev. A **37**, 4702 (1988).
- ²⁴ B.V.Chirikov, F.M.Izrailev and D.L.Shepelyansky, Sov. Scient. Rev. **2C**, 209 (1981).
- ²⁵ O.Bohigas, *Proceedings of the 1989 Les Houches Summer School on “Chaos and Quantum Physics”*, ed. M.J.Giannoni, A.Voros and J.Zinn-Justin, p.89, Elsevier Science Publisher B.V., North-Holland, (1991)
- ²⁶ K.M.Frahm and D.L. Shepelyansky, Phys. Rev. Lett. **79**, 1833 (1997).
- ²⁷ G.Casati, B.V.Chirikov, I.Guarneri and D.L.Shepelyansky, Physics Reports **154**,2 (1987).

¹ G.Casati, B.V.Chirikov, J.Ford and F.M Izrailev, Lecture Notes in Physics **93**, 334 (1979).

² R. Balescu, Phys. Rev. E **55**, 2465 (1997).

³ B.V.Chirikov, Phys. Rep. **52**, 263 (1979).

⁴ S.De Bievre and G.Forni, chao-dyn/9801003.

⁵ L.A.Bunimovich, Comm. in Math. Phys. **65**, 295, (1979).

⁶ F.Borgonovi, G.Casati and B.Li, Phys. Rev. Lett. **77**, 4744 (1996).

⁷ F.M.Izrailev, Phys. Rep., **196**, 299 (1990).